



ELSEVIER

UV-laser ablation of polyimide: from long to ultra-short laser pulses

B. Luk'yanchuk^b, N. Bityurin^c, M. Himmelbauer^a, N. Arnold^{a,*}^a *Angewandte Physik, Johannes-Kepler-Universität, A-4040, Linz, Austria*^b *General Physics Institute, Russian Academy of Sciences, 117942 Moscow, Russia*^c *Institute of Applied Physics, Russian Academy of Sciences, 603600, Nizhni Novgorod, Russia*

Abstract

Physical mechanisms of UV-laser ablation of polyimide (Kapton H) are discussed for different laser pulse duration from long (μs) to ultra-short (ps) laser pulses. Theoretical analysis of experimental data suggests that with long laser pulses the mechanism appears to be thermal. The activation energies for ablation are about 1.5 eV, and typical temperatures lie in the range 1400–1800 K. With ns pulses one can distinguish between the mass loss due to depletion of light volatile species from the bulk of the polymer, and the real ablation. The former is especially important near the ablation threshold. For sub-ps laser pulses ablation may proceed via preferential removal of electronically excited species. Here, decrease in delay time between two subsequent laser pulses may result in a decrease in ablation rate due to saturation and bleaching effects.

PACS: 81.15.Fg; 82.50.-m; 42.62.-b

Keywords: Laser ablation; Activation energies; Polyimide

1. Introduction

Although the UV-laser ablation of organic polymers was intensely investigated during the last 15 years (see [1], and references therein), the mechanisms of ablation are still not completely clear. The present paper is devoted to the UV-laser ablation of polyimide (PI) which is one of the most thermally and mechanically stable polymers, and its processing is attractive for many applications.

The main problem in the interpretation of the experimental data on UV-laser ablation kinetics is the lack of reliable in situ temperature measurements. Usually, the corresponding temperatures are estimated from the model calculations. The thermophysical and kinetic parameters of PI are hardly known for the typical ablation temperatures. Therefore, it is attractive to extract them from the experimental results, and to trace the influence of their changes onto the theoretical predictions.

The picture of ablation may vary with the duration of the laser pulse.

In the region of ultra-short laser pulses the net effect of the two pulses with near threshold fluences decreases with decreasing delay time between them [2].

The near threshold ablation kinetics of nanosecond laser pulses (7–30 ns) [3], and its theoretical analysis [4]

show, that the apparent activation energy is about 0.7 eV for the data at 248 nm. This is in contradiction with the good thermal stability of PI. At the same time, this kinetics does not follow the “photochemical law” typical for the direct bond breaking, at least with laser wavelength $\lambda \geq 248$ nm. If we consider thermal covalent bond-breaking (3–5 eV, [5]) mechanism of PI ablation, then high temperatures (about $(6-10) \times 10^3$ K), are necessary to reach the experimentally observed ablation rates. These temperatures are in contradiction with recent direct measurements [6] which reveal $T \approx 1660$ K for PI at 248 nm KrF-laser radiation.

In the region of long ns to μs laser pulses PI was successfully ablated in air by a single pulse of cw Ar⁺-laser light ($\lambda \approx 302$ nm) [7]. With sub-threshold conditions the surface was modified, which resulted in surface morphology changes [8]. The threshold fluence was found to depend on laser pulse duration. At the same time, experiments [9] did not reveal any significant difference in ablation kinetics for pulses with $\tau_p = 7$ and 300 ns (XeCl-laser at 308 nm).

Finally, with multiple irradiation by ~ 360 nm lines of cw Ar⁺-laser laser with dwell time in the ms range, the ablation (in vacuum) may become impossible [10]. Here, the carbon-rich residue (glassy carbon) was formed. All of the oxygen was eliminated from the polymer, mainly in form of CO molecules.

The small activation energies near the threshold may be associated with the thermal depletion of small volatile

* Corresponding author. Fax: +43-732-2468-9242; email: nikita.arnold@uk.uni-linz.ac.at.

fragments from the bulk of the PI. High rate of depletion may ultimately lead to a destruction of the polymer chain and a complete ablation of the polymer, while with the slow rate the recombination process may lead to the formation of almost a non-ablating residue. Within the ps pulse range, the photophysical mechanism with preferential ablation of excited species [11] may dominate. This mechanism is relevant for the ns range only if the thermal relaxation time is rather long. Among other factors which may play an auxiliary role are “weak bonds” [12], although their number is insufficient to provide the stationary ablation regime, and laser-induced stresses [13].

In the present paper we start with the analysis of long μs laser pulses using the AFM measurements of etched depth on PI ablated in air by cw Ar^+ -laser [7]. The theoretical analysis is done on the basis of stationary ablation model [14] combined with the measurements of the delay time for ablation at fixed laser intensity. It allows to estimate the apparent activation energy, enthalpy and the surface temperature. Analysis of the data shows, that the ablation kinetics is described well by the thermal model with activation energies of about 1.5 eV.

Then we show, that the depletion of light volatile species may be responsible for the Arrhenius tails in mass loss kinetics [3] for shorter laser pulses ($\tau_L \approx 15$ ns). This kinetics may be explained also by the photophysical model with relatively long thermal relaxation times.

Finally, we discuss the two-pulse ablation kinetics for the ultra-short laser pulses [2]. Here the role of electronic excitations becomes crucial.

2. Dependence of the ablation velocity on laser intensity stationary ablation regime

The conventional method to investigate the kinetics of laser ablation is to measure the thickness of ablated material, Δh , as a function of laser fluence $\phi = I_0 \tau_L$ for a fixed duration of the laser pulse, τ_L at sufficiently high intensity. If the thermal mechanisms play an important role in ablation, the dependence of ablated depth on laser pulse length at constant laser intensity I_0 provides a more convenient frame for the analysis of experimental results.

Let us assume that ablation has primarily thermal nature. Then, if the duration of the laser pulse is long enough, after a certain transition period the regime of stationary ablation [14,15] is reached. The meaning of the words “long enough” in this context is explained in Section 3. The characteristics of this regime can be found from the solution of the heat conduction equation and the temperature dependence of the material removal rate. The stationary heat conduction equation for the temperature T can be written in the coordinate system fixed with the ablation front as:

$$-vc\rho \frac{dT}{dz} = \frac{d}{dz} \left(\kappa \frac{dT}{dz} \right) + Q, \quad (1)$$

where κ is the heat conductivity, ρ density, and c specific heat (per unit mass) of the polymer, v is the stationary velocity of the ablation front. Q is the source term, which in the simplest case is given by the Bouguer law. Integrating (1) over z with boundary conditions at infinity

$$T|_{z=\infty} = T_\infty, \quad \text{and} \quad \left. \frac{dT}{dz} \right|_{z=\infty} = 0 \quad (2)$$

we find the first integral of the heat equation (energy conservation law):

$$AI_0 = \kappa \left. \frac{dT}{dz} \right|_{z=0} + H(T_s), \quad (3)$$

where $T_s = T(z=0)$ is the surface temperature, and A is the absorptivity of the material (we neglect screening by the plume). We also introduced the enthalpy of the solid phase: $H(T_s) = \int_{T_s}^{T_m} c(T) dT$.

The first term in r.h.s. of Eq. (3) can be found from the condition of the energy flux continuity. The flux of energy is given by the sum of the flux due to the heat conduction, and the energy transported by the macroscopic motion. The latter includes both the internal enthalpy and the kinetic energy of the moving media. Equating these fluxes at both sides of the ablation front (situated at $z=0$ in the moving coordinate system) one obtains (see also [14], and references therein)

$$-\kappa \left. \frac{dT}{dz} \right|_{z=0} - \rho v \left(H + \frac{v^2}{2} \right) = -\kappa_g \left. \frac{dT_g}{dz} \right|_{z=0} - \rho_g v_g \left(H_g + \frac{v_g^2}{2} \right), \quad (4)$$

where index g refers to the gas phase (plume), H and H_g are the enthalpies of the polymer and the gas (per unit mass), v_g is the gas velocity within the coordinate system fixed with the ablation front. The estimation shows, that for moderate laser intensities with subsonic velocities of ejected gaseous products, we can neglect terms $\propto v^2, v_g^2$, which are related to kinetic energies of the polymer and the gaseous products.

The thermal flux from the gas phase is negligible for the inert plume. If the chemical reactions take place within the plume (for example, post-oxidation in the air, secondary decomposition, etc.), this flux should be taken into account. We approximate this term as proportional to the mass flux:

$$-\kappa_g \left. \frac{dT_g}{dz} \right|_{z=0} = \rho v L_{\text{ch}} \epsilon, \quad (5)$$

where L_{ch} is the average heat effect of chemical reaction (for exothermal reactions $L_{\text{ch}} > 0$), and $\epsilon < 1$ gives the fraction of the energy which is transferred back to the surface of polymer.

Finally, we use the condition of the mass flux continuity, $\rho_g v_g = \rho v$, and assume for the difference in enthalpies of gas and solid phases:

$$H_g(T_s) - H(T_s) = L + \int_{T_\infty}^{T_s} c_g(T) dT - \int_{T_\infty}^{T_s} c(T) dT, \quad (6)$$

where L is the latent heat of material vaporization.

Using Eqs. (4)–(6) we can rewrite the energy conservation law (3) in the form convenient for further analysis:

$$AI_0 = \rho v \tilde{H}, \text{ with } \tilde{H}(T_s) \equiv L - \epsilon L_{ch} + \int_{T_\infty}^{T_s} c_g(T) dT. \quad (7)$$

Coefficient \tilde{H} may be considered as an apparent enthalpy, which characterizes the energy consumption in stationary one-dimensional ablation. Eq. (7) provides one relationship between v and T_s . The second one is given by the relation between the stationary ablation velocity and the surface temperature. We assume, that it has the Arrhenius behavior

$$v \equiv v(T_s) = v_0 \exp(-T_a/T_s), \quad (8)$$

where the preexponential factor v_0 is by the order of sound velocity in solid material [14]. Here, T_a may also be considered as an *apparent* activation temperature. Its usefulness will become clear in Section 4 where it is shown, that T_a remains constant in the broad range of experimental parameters.

At the first glance it seems that the two equations (7), (8) allow to obtain both the temperature T_s and the activation energy T_a if the dependence of the stationary ablation velocity v is measured as function of laser intensity I_0 . However, there are two intrinsic difficulties in this approach. First, the temperature dependence of \tilde{H} is not well known at high temperatures. Second, v in (8) is a very sharp function of temperature, which makes (7) and (8) practically independent, and (7) allows to determine \tilde{H} , while (8) allows to determine only the *ratio* T_a/T_s . In order to extract *both* T_a and T_s , additional experimental information should be used.

3. The delay time and the ablation threshold

Usually, the threshold of laser ablation is considered as threshold in fluence. If the laser intensity is fixed, the ablation occurs only if the duration of the laser pulse is long enough. The meaning of this delay in the thermal model, is that the material should be heated up to the temperatures when the ablation velocity (8) becomes significant. Before that, the surface temperature can be estimated from the time dependent solution F of the heat equation, which completely neglects ablation

$$T(z=0, t) = F(I_0, t). \quad (9)$$

In general, F depends on the temperature dependences of material parameters and surface modifications due to laser irradiation, which may make it non-linear with respect to

I_0 . As a simplest measure of the delay time t_v one can take the time, when the surface temperature given by Eq. (9) reaches its value in the stationary regime, T_s . In the subsequent analysis we employ for F the solution of the linear heat conduction equation with constant parameters [16]. This leads to an equation

$$T_s = T_\infty + \frac{AI_0}{\alpha\kappa} \left[\frac{2}{\sqrt{\pi}} \sqrt{D\alpha^2 t_v} + e^{D\alpha^2 t_v} \operatorname{erfc} \sqrt{D\alpha^2 t_v} - 1 \right]. \quad (10)$$

Here, α is the absorption coefficient and $D = \kappa/c\rho$ the heat diffusivity of the polymer. If the parameters of the material are known, and t_v is measured experimentally, (10) alone allows to estimate the temperature of stationary ablation T_s . Then, T_a and \tilde{H} can be determined from Eqs. (8) and (7) respectively, and the experimentally measured dependence $v(I_0)$.

There are several weak points in this simple procedure. One is obvious: the material and gas phase parameters are not well known at elevated temperatures. A more subtle question is related to the determination of t_v and its connection to the ablation threshold. In the picture presented above there is no ablation at $t < t_v$, before $T(z=0)$ reaches T_s , and after that ablation proceeds at a constant rate which corresponds to the velocity of the stationary ablation wave:

$$\Delta h(t) = \begin{cases} 0, & t < t_v \\ v(t - t_v), & t > t_v \end{cases} \quad (11)$$

Thus, t_v should be taken as an intersection point of the *linear interpolation* of the kinetic curves $\Delta h(t)$ with the time axis. In reality, this picture is oversimplified.

First, the ablation and/or surface modification (e.g., mass loss) starts before the temperature T_s is reached. Correspondingly, when $\Delta h(t)$ dependence becomes linear, a certain amount of material is already removed. This leads to an *underestimation* of t_v as determined from the slope of kinetic curves $\Delta h(t)$, in comparison with the time when T_s was reached in (10).

Second, in terms of relative deviations, the ablation velocity approaches its stationary value much slower than the temperature. This is due to strong exponential dependence in (8). Therefore, when the efficient material removal starts, the temperature is close to its value in the stationary wave, but the front velocity is still significantly smaller than its stationary value. This leads to an *overestimation* of the experimentally measured t_v with respect to the time when T_s was achieved in the heat conduction Eq. (10) without ablation.

The estimation of the influence of the first factor can be done by integration of $v(t)$ dependence in pre-stationary regime. The resulting thickness Δh_0 turns out to be small, and gives the correction of t_v of the order of $\Delta h_0/v(T_s)$ which is about 10% of t_v . The second factor works in

another direction and is more difficult to estimate. This was done on the basis of the model numerical calculations of non-stationary ablation. The resulting error is of the order of 20% of t_v for the numbers used in Section 4. Such an error in t_v leads to an about 10% error in T_s and correspondingly T_a , because in the region of relatively long pulses employed (PI is a strong absorber at this wavelength) $T_s \propto t_v^{1/2}$. Therefore, the accuracy of the experimental findings for T_s and T_a presented below is of the order of 10–15%. Some comments on t_v which are more specific for PI and the experimental arrangement employed are given in Section 4.

4. Ablation of PI by Ar⁺ laser at constant intensity

UV polymer ablation is usually done with excimer lasers. In the ns range the pulse duration of these lasers can hardly be varied, and the intensity during the pulse is by no means constant. Correspondingly, one cannot expect the stationary ablation regime [4]. Recently, new types of experiments have been performed [7]. Ablation was done in air by the cw Ar⁺-laser operating at the wavelength $\lambda = 302 \pm 4.5$ nm. This wavelength is close to $\lambda = 308$ nm for a XeCl excimer laser. The pulse duration ($140 \text{ ns} < \tau_p < 5000 \text{ ns}$) was controlled by an acousto-optic modulator. The intensity was varied within the range $54 \text{ kW/cm}^2 < I_0 < 430 \text{ kW/cm}^2$. The single-shot ablated profiles were measured by the atomic force microscope (AFM). The details of the experimental procedure are given in [7]. This experimental setup allows:

(•) to study the dependence of ablated depth on laser pulse duration at *constant* intensity,

(•) to avoid the attenuation of the incoming beam by ablated material. This is due to tight focusing ($\sim 4.2 \mu\text{m}$ diameter) and long pulses employed, which lead to a *three-dimensional* expansion of the vapors, so that only small fraction of ablated products contributes to the shielding of the surface,

(•) to measure *single-shot* depth profiles without recalculation of the ablated depth Δh from the mass loss measurements.

The single-shot ablated depths as functions of pulse length τ_p at different intensities are presented in Fig. 1. Straight lines approximate the kinetic curves in the linear regions. Strictly speaking, the dependence on pulse length does not necessarily coincide with the change of ablated thickness *during* the pulse because of the possible after-pulse ablation, and/or bulk modifications. Nevertheless, the expected errors are small and we will treat the kinetic curves in Fig. 1 as $\Delta h(t)$ dependences. One can see that ablation starts rather sharply, and then there exists a well defined linear increase in ablated depth with time. The absence of pre-stationary tails (sharp threshold) may be due to a hump formation observed at sub-threshold fluences [8]. In this region, the elevation of material may

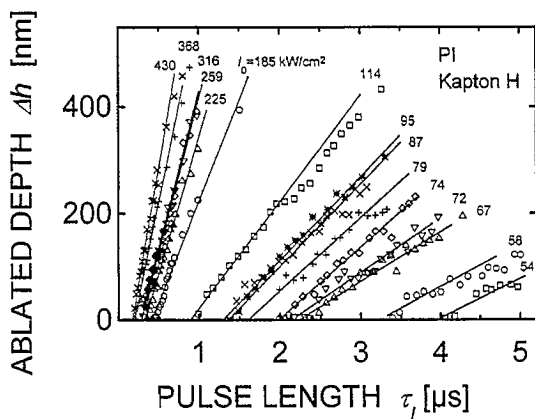


Fig. 1. The dependence of ablated depth on laser pulse duration for different values of laser intensity I_0 . Solid lines are linear interpolations of $\Delta h(t)$ dependences used for the determination of the stationary ablation velocity $v(I_0)$ and the delay time $t_v(I_0)$.

“cancel” the ablated depth. The decrease in the ablation rate for a given intensity observed at longer times is not expected in the stationary ablation model. One reason for it is the three-dimensionality (3D) of the heat flow which for the current setup, becomes noticeable after $\sim 3 \mu\text{s}$. For that reason the data at long times were not used in the linear fit (some of them are even not shown in Fig. 1).

Another reason may be the accumulated changes in the properties of material due to the loss of volatile species [13,17], carbonization [18], etc., which ultimately may lead to a formation of stationary regime but on the material *with modified properties* and correspondingly with different T_s and v .

The linear interpolation of the kinetic curves (solid lines) gives the stationary ablation velocities v and delay times t_v . They are shown as a function of laser intensity I_0 in Fig. 2. The solid line is the linear fit which corresponds to a value of $\bar{H} = 3.3 \text{ kJ/g}$ in Eq. (7). If we calculate the value of apparent enthalpy \bar{H} separately for each intensity, its value increases (up to 4.5 kJ/g) for smaller I_0 (i.e.,

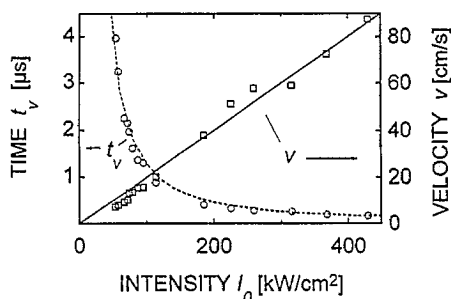


Fig. 2. The dependencies of stationary ablation velocity v (squares) and delay time t_v (circles) on laser intensity, derived from Fig. 1. Solid and dashed lines were calculated as described in the text.

longer pulses) as it can be seen from the squares lying below the solid line in Fig. 2. This is most probably due to the 3D heat conduction which starts to decrease T_s and v in this region. Another reason may be weaker heat flux from the plume for the long pulses (decrease in ϵ will increase \tilde{H} in (7)) due to the transport limitations for the chemical reactions in the gas phase. \tilde{H} changes with intensity even in the absence of these factors due to the $H_g(T_s)$ dependence in (7) (T_s is higher for higher intensities), but this dependence is weak and one can see, that the approximation $\tilde{H} = \text{const.}$ is justified, especially for shorter pulses.

Dashed line shows the $t_v(I_0)$ dependence calculated in the following way. All material parameters (including \tilde{H} , which is taken to be constant) are assumed to be known. Then, v is determined from (7), T_s from (8) and, finally, t_v from (10). The material parameters used in this and subsequent calculations are: $\rho = 1.42 \text{ g/cm}^3$, $D = 7.5 \times 10^{-4} \text{ cm}^2/\text{s}$, $T_\infty = 300 \text{ K}$, $A = 0.89$, $v_0 = 10^6 \text{ cm/s}$, $c = 2 \text{ J/gK}$, $\tilde{H} = 3.3 \text{ kJ/g}$, $T_a = 1.65 \times 10^4 \text{ K}$, $\alpha = 1.5 \times 10^5 \text{ cm}^{-1}$. \tilde{H} is determined from Fig. 2, and T_a from Fig. 3 below. This single set of parameters describes $t_v(I_0)$ dependence quite well.

From the experimentally derived values of $t_v(I_0)$ one can calculate T_s for each I_0 according to (10). Note, that this does not require the knowledge of T_a and v_0 and any information about the stationary regime. The result is shown in Fig. 3 by the circles. In the regime of big intensities there is an increase in $T_s(I_0)$ which should hold for the stationary ablation. The increase of T_s at small I_0 (long pulses) can be explained if the 3D heat conduction is taken into account.

When v is measured, and T_s is recalculated for each I_0 we determine T_a from Eq. (8) (Fig. 3, squares). T_a is not directly proportional to T_s because v increases with I_0 . As a result, T_a is almost constant (especially for shorter pulses) which is an indication of a thermal nature of underlying processes and demonstrates the consistency of the approach. Namely, if the wrong values of the material

parameters are taken, the dispersion in the calculated T_a values is much bigger. The question about the values of material parameters at elevated temperatures is a crucial one, because T_a is determined mainly by the ratio T_a/T_s which enters the exponent in (8). The values of c , D , and α are chosen in the way which provides for T_s and T_a the estimation from above if no significant modification of material is assumed. For example, c has the highest measured value for PI (at 700 K, [2,3]) which is still smaller than its value expected at the temperatures of ablation. The highest reported value of α at 302 nm [1] was taken. 1.3 times increase in the specific heat c (with κ kept constant), or 1.5 times decrease in α , or 3 times decrease in v_0 reduce the calculated T_a by about 15%. The obtained value is $T_a \approx 1.65 \times 10^4 \text{ K} \approx 1.5 \text{ eV}$.

Let us briefly address the question about the microscopic mechanisms of ablation. The destruction of the PI chain may proceed via the elimination of 2 to 5 CO molecules per monomer [1,10,12]. Thermogravimetric measurements suggest for these decarbonylization reactions the activation energies in the range 1.6–3.7 eV [12]. When one of the CO molecules is lost, the polymer chain may either replace the produced defect by a stronger bond, or loose the CO molecule from the same imide ring. In the latter case the polymer chain is cut, and (if the surface concentration of such cuts is high enough) the ablation of the heavy fragments (with sizes of a few monomers) becomes possible. If the rate of CO depletion is slow, essential modification of material may take place. With ms pulses the formation of glassy carbon was reported [19].

Additionally, so-called "weak bonds" always exist in real polymers due to the presence of defects of different kinds. They may cause mass losses in PI heated above 600 K. The number of weak bonds is insufficient to provide the developed ablation. Under certain conditions the ablation may be facilitated by the laser induced stresses [13].

5. Kinetic curves and threshold at fixed laser pulse length

When the kinetic parameters of ablation are deduced from the experiments with constant intensity, we can explain the kinetic curves $\Delta h(\phi)$ measured at a constant pulse length τ_p . We employ formula (11) where for each fluence ϕ stationary velocity is calculated from (7) with $I_0 = \phi/\tau_p$ and then t_v is calculated from (10) with T_s recalculated from v using (8). The resulting fit for ablation at $\tau_p = 1000 \text{ ns}$ is shown in Fig. 4 by solid line, together with experimental points for other pulse lengths. The value $\tilde{H} = 3.3 \text{ kJ/g}$ was employed. With fixed \tilde{H} the fit is somewhat worse for other τ_p . If slightly different \tilde{H} are taken for different τ_p , according to Fig. 2, the fit becomes perfect for all curves. One can see that the $\Delta h(\phi)$ curve is almost linear. The derivations from linearity are due to the $t_v(I_0)$ dependence in (11).

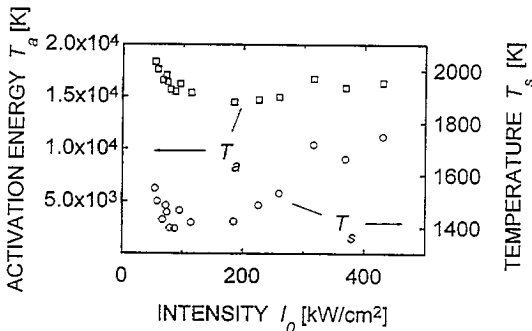


Fig. 3. The temperature of stationary ablation T_s (circles) and the activation energies T_a (squares) calculated from t_v and v depicted in Fig. 3.

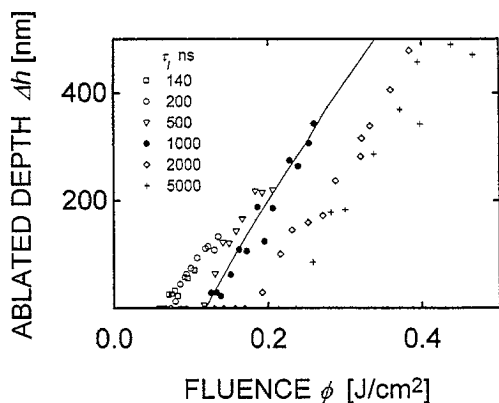


Fig. 4. Kinetic curves of ablated depth versus laser fluence for different pulse durations. The solid line was calculated with $\bar{H} = 3.3$ kJ/g.

From the experimental plots in Fig. 4 one can clearly see the dependence of the threshold fluence ϕ_{th} on pulse duration. Corresponding values reported by different groups are shown in Fig. 5. Note, that the data from [9,19–21] are obtained at slightly different wavelength ($\lambda = 308$ nm) with XeCl excimer laser. Therefore, the absorption coefficient and the temporal profile of the laser pulse were somewhat different. The solid line was calculated from the simultaneous solution of Eqs. (7), (8), (10) with respect to ν , T_s , and I_0 , with $t_v = \tau_p$ at the threshold. After that threshold fluence was taken to be $\phi_{th} = I_0 \tau_p$. One can see an increase in ϕ_{th} with τ_p due to the necessity to heat thicker volume of material for lower intensities. In the region of short ns pulses, the thermal model, like the purely photochemical one, predicts ϕ_{th} almost independent on τ_p . The region where the distinctions between the two starts, is given by the condition $D\alpha^2 \tau_p \geq 1$, and thus shifts

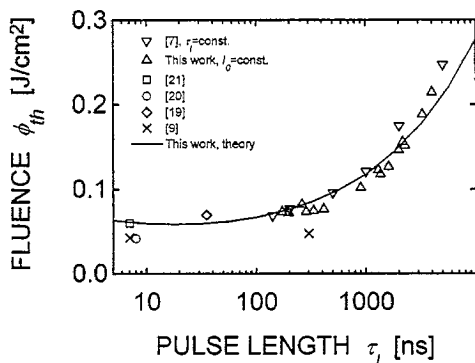


Fig. 5. The dependence of threshold fluence on pulse duration taken from different references. Up triangles: thresholds derived from the linear interpolations in Fig. 1. Down triangles: threshold taken from the experiments at fixed τ_p (Fig. 4). The solid line was calculated for a thermal model as described in the text.

to even longer τ_p for the polymers which are weaker absorbers.

6. Laser ablation with nanosecond pulses

If in analogy to the models of laser evaporation of metals [14], one describes the polymer ablation as surface sublimation process, the corresponding activation energies are expected to be of the order of covalent bonds breaking energies ~ 3 eV. [5,15,22]. The attractiveness of such kind of approach is the universality of description, i.e., the model is free of details of chemical reactions within the polymer and may be applied to a wide variety of polymer materials.

The analysis of single shot experiments [3], however, gave the value of activation energy in polyimide below ~ 1 eV. To explain the thermal stability of the PI with such small activation energies, the surface evaporation model was then converted into the photophysical surface ablation model [11] which takes into account that electronically excited macromolecule needs significantly smaller activation energy to be decomposed than the molecule in the ground state. Such a decrease in excited bond energies is typical for many organic molecules [23]. In this picture, laser ablation proceeds thermally, mainly via the photo-excited channel. This model has been applied to quantitative description of ablation kinetics for ns laser ablation of PI [4,11,13]. Note, that the experiments with nanosecond pulses are performed with much higher intensities than it was considered in the previous section. The experimental data may be fitted with high accuracy, if the thermal relaxation time t_T is by order of few hundred picoseconds. It is one order of magnitude higher than value $t_T \approx 36$ ps measured in [24] by pump-probe technique for the radiation of 3-rd harmonic of Nd-laser, ($\lambda = 355$ nm). If these findings hold also for shorter wavelengths, the photochemical mechanism is more relevant for ps laser pulses. For laser pulses long in comparison with t_T the consideration of excited species does not change the thermal nature of the ablation process, but rather makes the preexponential factor ν_0 in (8) proportional to laser intensity.

The other possibility to describe the nanosecond single-shot experiments is to consider the bulk effects. Similar effects were studied in connection with sub-threshold PMMA modification and etching [25–27]. The simplest model [13,17] for PI takes into account the creation of small molecules within the bulk of the material due to splitting them off the polymer chains. In this picture one distinguishes between the mass-loss, which is measured by microbalance technique [3], and real ablation which causes the hole formation measured by the AFM. Overall mass-loss is caused by both elimination of small molecules produced within the bulk of material, and by the layer by layer material removal (“real ablation”). The activation energies of these processes may be different.

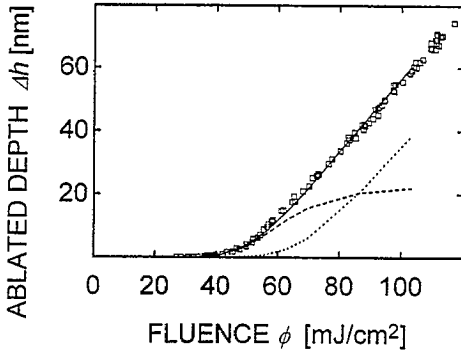


Fig. 6. Model calculations for the mass loss experiments [3] on PI Kapton with XeCl laser, $\lambda = 308$ nm. The total mass loss (solid line) is the sum of mass loss due to the depletion of light species from the bulk (dashed line), and real surface ablation (dotted line).

Their absolute values depend strongly on the assumptions about the high-temperature behavior of the thermophysical properties of the material. With D and other parameters kept constant, the calculated T and T_a are almost inversely proportional to the (volumetric) specific heat ρc . In calculations [17] the room temperature value of the specific heat $c = 1.1$ J/gK was used. Correspondingly, if $c = 2$ J/gK is used, these activation energies should be reduced by a factor of two, to become ~ 0.8 eV for the pre-threshold mass loss, and ~ 1.5 eV for the ablation itself in agreement with the results of Section 4. Note, that ρc may also change due to the changes in density of the modified material. With long pulses this effect may be very pronounced [10].

The thermal destruction experiments [12] (thermogravimetry) performed in vacuum at a slow heating rates, also reveal for polyimides two activation energies. The small activation energy (0.5–1 eV) for the temperatures around 750 K, and higher activation energy (2–4 eV) for somewhat higher temperatures (~ 1000 K). Fig. 6 shows the explanation of mass loss experiments [3] (PI Kapton, XeCl laser, $\lambda = 308$ nm) within the framework of the model with bulk processes. The kinetic curves within the sub-threshold region can be explained by the removal of light volatile species from the bulk of the material (dashed line), while above the threshold the total mass loss (solid line) is mainly determined by the real surface ablation (dotted line).

Thus, both models, namely, the photophysical model with the thermal relaxation time $t_T \approx 500$ ps, and the thermal model which incorporates the bulk processes, are able to describe the single-shot experiments [3]. The discrimination between the two should be done on the basis of the direct measurements of the relaxation times.

7. Effect of ultra-short laser pulses

In the region of ultra-short laser pulses (USLP), where the duration of the laser pulse τ_p is comparable with the

thermal relaxation time t_T , one should take into account the high level of electronic excitations and corresponding changes in material properties. First of all, these are the optical properties, such as absorption and reflection. But the mechanism of material removal itself may also be influenced by excitations. One way to take this into account is the photophysical model of UV laser ablation [4,11], where the activation energy for material removal in electronically excited state was assumed to be smaller, than that in the ground state.

Let us discuss the experimental results [2]. Here, two sub-ps pulses (KrF laser, $\lambda = 248$ nm) affected PI. Both were of the same fluence, 25 mJ/cm² (which is slightly above the ablation threshold), and the delay time between them was varied from 0 to 200 ps. It was shown, that the net effect of two pulses *decreases with decreasing delay time*. Below we present the numerical results on ablation kinetics for this arrangement, based on the purely thermal model and on the photophysical model. In both models we assume the relaxation time $t_T = 30$ ps, which is close to the value reported in [24].

The corresponding equations can be written in analogy to [4] for both of the considered models. They include the heat conduction equation, kinetic equation for the concentration of excited species N^* , and the equation for intensity distribution. In both models the transient changes in optical properties caused by the electronic excitations were described on the basis of generalized four-level system [4]. In this scheme absorption from the ground state is characterized by the cross section σ_{01} , and the sequential absorption channel by σ_{12} . The ratio of these cross sections $s = \sigma_{12}/\sigma_{01}$ was introduced to describe bleaching ($s < 1$) and darkening ($s > 1$) effects. This parameter enters the equation for the intensity distribution and the heat conduction equation (for details see [4]). For the thermal model the ablation velocity is given by (8). For the photophysical model the expression for the ablation velocity is modified in order to take into account the difference in ablation rates for the species in the ground state and in the excited state [11]:

$$v = \left(1 - \frac{N_s^*}{N}\right) v_A \exp(-T_a/T_s) + \frac{N_s^*}{N} v_A^* \exp(-T_a^*/T_s). \quad (12)$$

Here, T_a and T_a^* are the activation energies (in K) for the ground state and the excited state, respectively. The subscript s (not to mix with the parameter s introduced above) refers as before to the ablation front at $z = 0$. The boundary conditions for the heat equation take into account possible differences in enthalpy of ablation from the excited and non-excited channel in the form similar to (12). The plume was assumed to attenuate the incident radiation with the absorption coefficient α_p (recalculated to the depth of ablated material). The possible induced changes in reflection coefficient were neglected.

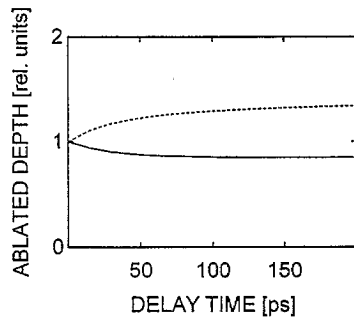


Fig. 7. The calculated dependence of ablated thickness on the delay time between the pulses in a two-pulse experiment. Calculations are done for the thermal model. Solid line: bleaching ($s = 0$); dashed line: darkening ($s = 3$). Ablated depth is normalized to its value for zero delay time.

We investigate the dependence of ablated depth on delay time between identical pulses. The results of the calculations are shown in Fig. 7 for purely thermal model (with $T_a = 1.5 \times 10^3$ K \equiv 1.3 eV, which is smaller than the bond breaking energy). The evaporation enthalpy was also decreased proportionally. In Fig. 8 the results for the photophysical model with the same values of parameters (apart from t_T) as in [4] are presented. The changes in parameters, such as activation energy, evaporation enthalpies, influence the absolute value of the etched depth, but not the qualitative picture.

In the thermal model, for the case of bleaching ($s = 0$, solid line in Fig. 7) the ablated depth increases with decreasing delay time. This is because bleaching increases the heated volume. For the case of darkening ($s = 3$, dashed line) the ablated depth decreases with decreasing delay time. It may be connected with the overheating of surface layers as it was argued in [2].

In contrast, for the photophysical model in the case of bleaching ($s = 0$, solid line in Fig. 8) the etched depth decreases with decreasing delay time. With the numbers employed, even the induced darkening ($s = 3$, dashed line) does not reverse this trend. The physical reason for this

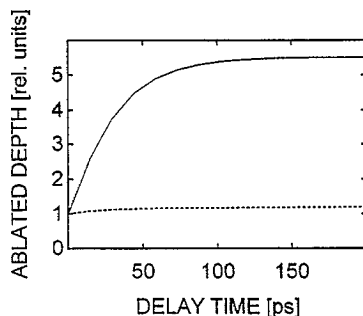


Fig. 8. The same as in Fig. 7, but for the photophysical model. Solid line: bleaching ($s = 0$); dashed line: darkening ($s = 3$).

effect can be explained in the following way. For the photophysical model the evaporation of excited species (second term in (12)) dominates. Here, the first pulse heats material, while the second one electronically excites the heated region, which causes efficient ablation. Due to saturation effect, which is essential under the current conditions, the optimal regime is realized, when all the excited species produced by the first pulse relax and thus produce maximal possible heating before the action of the second pulse.

These considerations indicate, that the experimentally observed dependences may be explained in different ways, and thus demand more accurate analysis.

8. Conclusions

We have studied the influence of different physical mechanisms on the ablation of polyimide (Kapton H) by the UV laser light.

With long (0.1–5 μ s) cw Ar⁺-laser pulses at $\lambda = 302$ nm, the mechanism appears to be thermal. The parameters of ablation are obtained from the analysis of the ablation kinetic curves at constant intensity. The apparent ablation enthalpy somewhat decreases for shorter laser pulses, probably due to the energy released in the exothermal reactions in the air, which involve primary ablation products. Calculated ablation temperatures are in the range 1400–1800 K. The apparent activation energies lie in the region around 1.5 eV. The reason for that may be the loss of gaseous CO. The elimination of two carbonyl groups from the same imide ring may lead to the cut of polymer chains which allows the ablation of the rest of material. With slower CO depletion rates in ms laser pulses, the polymer chains may recombine into non-ablating carbon-rich residue [10].

With short ns pulses one can distinguish between the mass loss, which is due to depletion of light volatile species from the bulk of the polymer, and the real ablation which leads to an ablated crater formation. The mass loss is especially important near the ablation threshold and probably proceeds with lower activation energy than the real ablation.

For the ps and fs laser pulse duration, the finite thermal relaxation time and the photophysical effects start to play an important role. The decrease in time delay between two USLP produces a decrease in ablation rate. This can be explained either by the thermal mechanism with darkening or by the photophysical mechanism with bleaching effects.

Acknowledgements

We wish to thank Prof. D. Bäuerle, Dr. E. Arenholz and Prof. S. Anisimov for helpful discussions and the

Fonds zur Förderung der Wissenschaftlichen Forschung in Österreich for financial support. Part of this work was supported by the Russian Basic Research Foundation grant 96-02-18941, and by INTAS (grant 94-902).

References

- [1] R. Srinivasan, in: *Laser Ablation. Principles and Applications*, ed. J.C. Miller, Springer Ser. Mater. Sci. Vol. 28 (Springer, Berlin, Heidelberg, 1994) p. 107;
E. Sutcliffe and R. Srinivasan, *J. Appl. Phys.* 60 (1986) 3315.
- [2] S. Preuss, M. Späth, Y. Zhang and M. Stuke, *Appl. Phys. Lett.* 62 (1993) 3049.
- [3] S. Küper, J. Brannon and K. Brannon, *Appl. Phys. A* 56 (1993) 43.
- [4] B. Luk'yanchuk, N. Bityurin, S. Anisimov, N. Arnold, D. Bäuerle, *Appl. Phys. A* 62 (1996) 397;
B. Luk'yanchuk, N. Bityurin, S. Anisimov, D. Bäuerle, in: *Excimer Lasers*, ed. L.D. Laude, NATO ASI Series, Vol. E 256 (Kluwer, Dordrecht, 1994) p. 59.
- [5] J. Guillet, *Polymers — Photophysics and Photochemistry. An Introduction to the Study of Photoprocesses in Macromolecules* (Cambridge University Press, Cambridge, 1985).
- [6] D.P. Brunco, M.Q. Thompson, C.E. Otis, P.M. Goodwin, *J. Appl. Phys.* 72 (1992) 434.
- [7] M. Himmelbauer, E. Arenholz, D. Bäuerle, *Appl. Phys. A* 63 (1996) 87.
- [8] M. Himmelbauer, E. Arenholz, D. Bäuerle and K. Schilcher, *Appl. Phys. A* 63 (1996), to be published.
- [9] R.S. Taylor, D.L. Singleton, G. Paraskevopoulos, *Appl. Phys. Lett.* 50 (1987) 1779.
- [10] R. Srinivasan, R.R. Hall, W.D. Loehle, W.D. Wilson, and D.C. Allbee, *J. Appl. Phys.* 78 (1995) 4881.
- [11] B. Luk'yanchuk, N. Bityurin, S. Anisimov, D. Bäuerle, *Appl. Phys. A* 57 (1993) 367.
- [12] M.I. Bessonov, *Polyimides — a Class of Thermally stable Polymers*, NASA Technical Memorandum, Washington, D.C., 1986), (Translated from Russian: Poliimidy — Klass Termostoikikh Polimerov, Nauka, Leningrad, 1983); W.W. Wright, in: *Developments in Polymer Degradation — 3*, ed. N. Grassie (Applied Science Publishers, London, 1981) p. 1.
- [13] B. Luk'yanchuk, N. Bityurin, S. Anisimov, A. Malyshev, N. Arnold, and D. Bäuerle, *Appl. Surf. Sci.* (1996), to be published.
- [14] S.I. Anisimov, Ya.A. Imas, G.S. Romanov, Yu.V. Khodyko, *Action of High-Power Radiation on Metals* (National Technical Information Service, Springfield, VA, 1971).
- [15] D. Bäuerle, B. Luk'yanchuk, P. Schwab, X.Z. Wang, and E. Arenholz, in: *Laser Ablation of Electronic Materials*, ed. E. Fogarassy and S. Lazare, Vol. 4 (North-Holland, Amsterdam, 1992) p. 39.
- [16] D. Bäuerle, *Laser Processing and Chemistry*, 2nd Ed. (Springer, Berlin, 1996).
- [17] M. Himmelbauer, N. Bityurin, B. Luk'yanchuk, N. Arnold, and D. Bäuerle, (NLMI-96), to be published in *Proc. SPIE*.
- [18] H.M. Phillips, S. Wahl, and R. Sauerbrey, *Appl. Phys. Lett.* 62 (1993) 2572.
- [19] J.H. Brannon, J.R. Lankard, A.I. Baise, F. Burns, J. Kaufman, *J. Appl. Phys.* 58 (1985) 2036.
- [20] P.E. Dyer, J. Sidhu, *J. Appl. Phys.* 57 (1985) 1420.
- [21] J.E. Andrew, P.E. Dyer, D. Forster, P.H. Key, *Appl. Phys. Lett.* 43 (1983) 717.
- [22] S.R. Cain, F.C. Burns, C.E. Otis, and B. Braren, *J. Appl. Phys.* 72 (1993) 5172.
- [23] V.G. Plotnikov, *Dokl. Akad. Nauk SSSR* 301 (1988) 376.
- [24] J.K. Frisoli, Y. Hefetz, T.F. Deutsch, *Appl. Phys. B* 52 (1991) 168.
- [25] A.A. Babin, N.M. Bityurin, A.V. Polyakov, F.I. Feldchtein and N.L. Khvatova, *Laser Phys.* 2 (1992) 805.
- [26] N. Bityurin, *Abstracts of Int. Conf. ICPEPA-2, Jerusalem, Israel* (1995) p. 102.
- [27] N. Bityurin, S. Muraviov, A. Alexandrov and A. Malyshev, *Appl. Surf. Sci.* (1997) to be published.